ADVANCED TECHNOLOGIES AND MATERIALS VOL. 43, NO. 1 (2018)
DOI: 10.24867/ATM-2018-1-003

ADVANCED
TECHNOLOGIES
& MATERIALS

Impact energy properties of weld joint of high-hardness armor steel

Aleksandar Čabrilo,* Katarina Gerić

University of Novi Sad, Faculty of technical sciences, Novi Sad, Serbia

ABSTRACT

Welding of armored steel is complicated by the high percentage of carbon in the base metal, the presence of faults in the form of cracks and pores that occur in the weld metal and heat affected zone (HAZ) during the welding process. The crack formed in base metal or HAZ, due to dynamic or impact loads, can easily continue to propagate to the fusion line, after which its accelerated growth may occur. It was demonstrated that the selection of the preheating and interpass temperature is important in terms of the cooling rate and quantity of diffusible and retained hydrogen in the weld joint. Due to the significant interest in quantifying the resistance of material to initiation and propagation of cracks, the impact energy was measured with instrumented pendulum in the zone of base metal, weld metal and HAZ, at temperatures of -40 °C, -20 °C, 0 °C and 20 °C. The impact energy tests showed high energy for initiation as well as crack propagation in weld metal and HAZ zones, while the lowest energy was in the base metal.

Key words: *GMAW welding, armor steels, austenitic stainless steel, instrumented Charpy tests.*

1. INTRODUCTION

Armor steel belongs to the ultra-high tensile strength and hardness group of steels. Welding of armor steel is complicated due to the high percentage of carbon content in the base metal and the presence of faults in the form of cracks and pores in the weld metal zone, whereby fractures may be initiated in the weld metal [1].
Austenitic filler material is traditionally used for armor steel welding because of hydrogen dilution improved in an austenitic phase [2]. After the welding process, solidification cracking may result from high thermal expansion of the austenitic stainless steel and invisible defects may be created in the weld metal zone.
For heavy structural engineering, such as armored military vehicles frequently being under the effects of impact and variable loads, mechanical properties of welded joints and the weld metal zone must be known. Due to variable loads, cracks created in the weld metal may easily propagate towards the sensitive fusion line (FL), followed by their possible rapid growth. The impact load is critical for armored vehicles, so the determination of the impact energy required for crack initiation and growth made by instrumented pendulum with Charpy V specimens, is very significant, [3].

For armored vehicle structures safe and rational dimensioning, it is necessary to know dynamic effects extreme values and time periods. Therefore, there is a significant interest in material resistance related to crack initiation and propagation. For the armored military vehicles reliable operation, it is very important to be able to carry out a good risk assessment of existing crack type faults. Although austenitic filler material is used the most frequently for welding and has several unusual features including its high manganese content, few articles consider the problem of its mechanical properties.
The main goal of this study was to investigate the impact energy by instrumented pendulum in welded joint. Fracture surfaces for the impact energy were also investigated by Scanning Electron Microscope (SEM). Subsequently, samples in the weld metal region were studied by tensile strength test, hardness measurements, metallography and chemical analysis.

2. MATERIAL AND EXPERIMENT

2.1. Base and filler material

Gas metal arc welding (GMAW) and AWS ER307 solid wire is used for welding armor steel Protac 500. Welding

* *Corresponding author's.e-mail: cabrilo@uns.ac.rs*

direction is parallel to the rolling direction, as shown in Fig. 1. Cold rolled plates 12 mm thick are cut to the required dimensions (250 x 100 mm), while V joint under the angle of 55° is prepared by Water Jet Device. Robot Kuka and Citronix 400A device was used during the welding process testing, [4]. Robotic welding is used for human factor effect elimination, in order to allow a fine adjustment of parameters and results repeatability.

The chemical composition (wt. %) of the base metal, armor steel, was 0.27 C, 1.07 Si, 0.706 Mn. 0.637 Cr, 1.09 Ni, 0.3 Mo, 0.039 V, 0.01 S, and 0.02 P. The chemical composition (wt. %) of the filler material, Mn type stainless steel, was 17.76 Cr, 8.24 Ni, 6.29 Mn, 0.89 Si, and 0.08 C. The chemical composition of the welded joint after the welding process was obtained by an ARL 2460 spectrometer, [4].

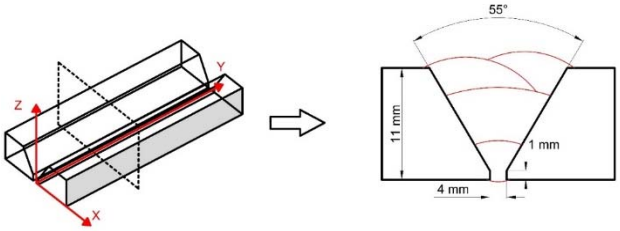

Fig. 1. *Schematic drawing of edge preparation and welding configuration.*

The welding parameters are shown in Table 1. The welding was performed in four passes (Fig. 1). GMAW welding was performed in a shielding gas of Ar + 2.5% CO_2 with flow rates of 10 $^{L}/_{min}$ times the wire diameter and 12 $^{L}/_{min}$ times the wire diameter. The wire diameter was 1.0 mm.

Table 1. – *Welding parameters for manual and automated welding of Protac 500 armor steel.*

Pass		***1***	***2***	***3***	***4***
Filler material	ER 307				
Preheat and interpass temperature	[°C]	150	160	160	160
Current	[A]	168	215	215	215
Voltage	[V]	16.sep	25.maj	25.maj	25.maj
Wire speed	[$^{m}/_{min}$]	7.apr	12.sep	12.sep	12.sep
Welding speed	[$^{m}/_{min}$]	0.16	0.15	0.29	0.29
Heat input	[$^{kJ}/_{mm}$]	jan.13	feb.19	jan.13	jan.13
Shielding gas	Ar.+ 2.5%CO_2				

For more detailed analysis of the selected welding parameters, the testing included the quantity of diffused hydrogen in the zone of the weld metal. Tests used the method of hot gas extraction (CGHE), while the quantity of hydrogen was measured by gas chromatography. The measurement of the diffused hydrogen quantity was performed according to EN ISO 3690 [5]. Before testing, the device was calibrated with a known quantity of hydrogen. The plate on which the welded pass was to be applied was preheated to 150 °C to simulate the real welding conditions. The filler material with the welding parameters shown in Table 1 was applied after being preheated and placed into a copper clamp, where the copper plate was positioned under the plate and test specimens. The testing process was repeated at 160 °C to test the impact of the interpass temperature on the quantity of diffused hydrogen. Three measurements were taken at each of these preheating temperatures, and the mean value was taken as the result.

The microstructural examination was performed using a "Leitz – Orthoplan" metallographic microscope and a scanning electron microscope JEOL JSM 6460LV at 25 kV. The samples were ground using SiC papers, polished with a diamond paste and finally etched with a mixture HCl and HNO3 in weld metal region, and 3% HNO3 reagent to reveal the structure of base metal. Microhardness distribution from top to bottom along the centerline of the weld was measured for the purpose of welded metal characterization. Digital Micro Vickers Hardness Tester HVS 1000, Laiznou Huayin Testing Instrument Co, under the load of 500 g, was used in order to measure microhardness.

Tensile tests were performed according to the standard EN ISO 4136 [6]. A water jet cutting machine was used for specimen preparation. Tensile strength tests were performed on a servo-hydraulic tension testing machine, Instron 8033, using a strain rate of 0.125 $^{mm}/_{s}$.

Charpy impact tests in base metal, heat affected zone and weld metal, were performed on specimen's size 10 x 10 x 55 mm, with V notch of 2 mm three time set least for each datum point at: 20 °C, 0 °C, -20 °C and -40 °C. Load-displacement curves were obtained from the instrumented Charpy impact system attached in to the impact tester. After the test, fracture surface were examined by a SEM to observe fracture modes.

3. RESULTS

3.1. Nondestructive testing (NDT)

The welded joints were free of pores and cracks in all zones. Visual and radiographic testing showed that the welded joints were of class B quality, according to EN ISO 5817 (2015) [7]. The welded joint was uniform along the weld metal length due to constant welding parameters, gun orientation, and positioning throughout the process.

The results of radiographic testing is shown in Fig.2, revealing that the obtained welded joint had no cracks. The results of welding show a joint without porosity (Fig,2).

The quantity of hydrogen measured by hot gas extraction is shown in Table 2. A higher quantity of hydrogen in the welded joint represents a higher risk of hydrogen brittleness, which, in turn, affects the welded construction lifetime. The presence of hydrogen in the weld metal may also have a negative effect on the mechanical properties.

The results of diffused hydrogen testing is shown in Table 2. Nearly identical values have been obtained for preheating temperatures of 150 °C and 160 °C. The

slightly lower quantity obtained for 160 °C can be explained by the fact that the quantity of diffused hydrogen decreases with increasing temperature.

Fig. 2. *Results of RT testing of welding process of high hardness armour steel.*

Table 2. – *Quantity of diffused and residual hydrogen.*

Temperature/type of hydrogen testing	***Diffused hydrogen testing***	
	Preheating temperature 150 °C	Interpass temperature 160 °C
	ml/100 gr	ml/100 gr
400	0.12±0.09	0.11±0.085

3.2. Hardness

The weld metal micrograph Fig. 3 a) consist of austenite with delta ferrite. Delta ferrite becomes finer at lower heat input and cooling rate. The content of delta ferrite measured by Feritscope: in the weld root 11.7%, in the center 5.4%, in the upper part 3.2%. The base metal micrograph Fig. 3 b) in quenched and tempered condition consists of tempered and quenched martensite within the range of hardness 480-540 HB which is within accepted criteria of standard, MIL-STD-1185, [8].

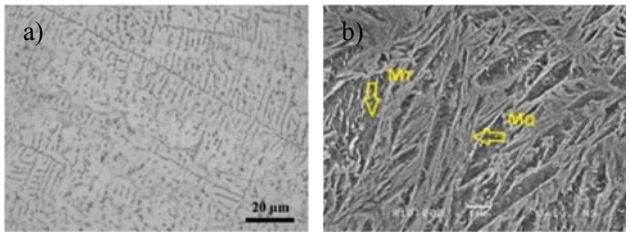

Fig. 3. *a) Optical micrograph of AWS ER 307 filler, Fig. 3. b) SEM micrograph of base metal. MT - tempered martensite, MQ - quenched martensite*

Hardness rises from the center of the weld metal (WM) (190 HV), to the line of fusion and along the line on WM side has a value of 339 HV, Fig.4-a). The hardness is growing in the HAZ zone and reaches a maximum value of 521 HV, at a distance of 8 mm from the weld metal axis. After a maximum, the hardness trend is in decline with the achieved minimum hardness of 378 HV, at a distance of 10 mm from the weld metal axis. The hardness then grows and ends at a distance of 14 mm from the weld metal axis with a value of about 509 HV. The distance of 14 mm is also the limit of HAZ and base metal. The BM hardness value is 509 HV. The hardness was measured also longitudinally along the width zone of 0.5 mm following fusion line. Results from Fig.4-b) show that fusion line hardness does not exceed 442 HV, which is very good for this zone. Hardness falls from the bottom to the upper zone, which can be the result of the heat effect that is higher in zones closest to the last passage than it is in the root passage, which is certainly affected by the already cooled additional and base metal.

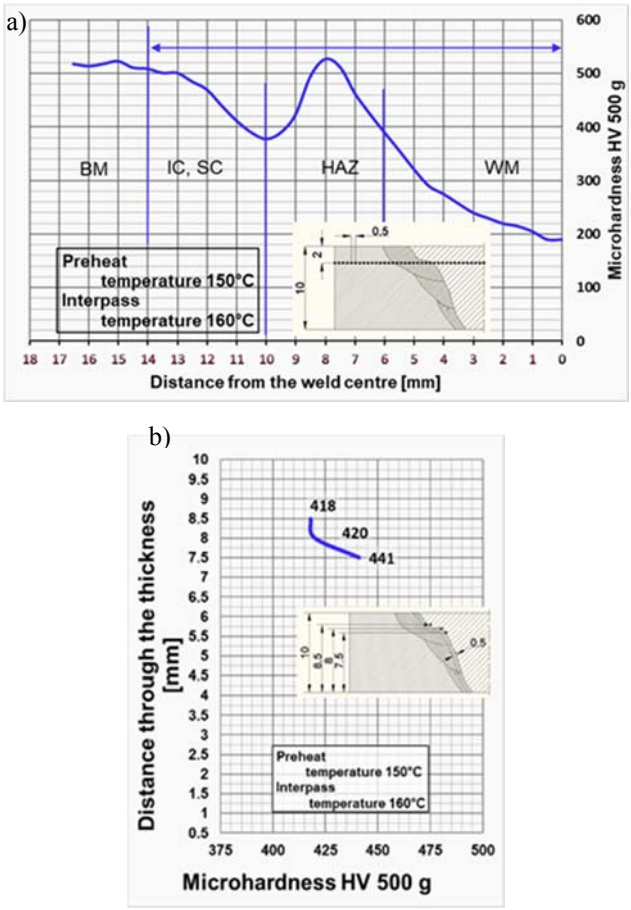

Fig. 4. *a) Optical micrograph of AWS ER 307 filler, Fig. 4. b) SEM micrograph of base metal. MT - tempered martensite, MQ - quenched martensite.*

3.3. Tensile characteristics

While tensile characteristics were being tested, a fracture appeared in the weld metal. The tensile strength was 833 MPa, while the yield strength of 552 MPa was within the expected limits. The difference between tensile and yield strength was 311 MPa, indicating a high ductility of the weld.

Fig.5 a) and b) shows the fracture surfaces of the weld metal region, which reveals that many smaller dimples mixed with several larger dimples are distributed on the fracture surfaces. The formation of large dimples is related to brittle particle fracturing and particle–matrix

decohesion. The weld metal chemistry shows 8.19 (wt. %) nickel content. A higher nickel content increases the toughness in fully austenitic compositions.

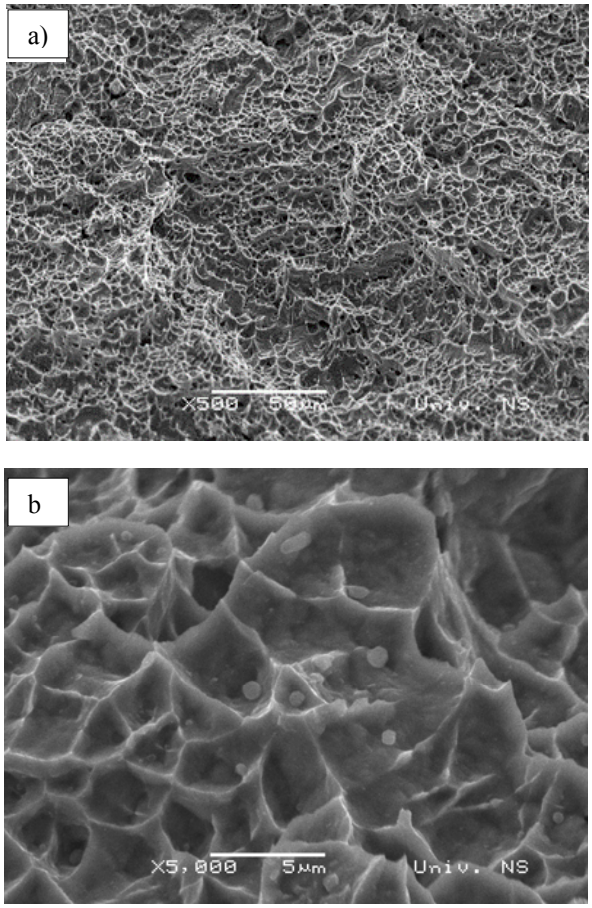

Fig. 5. *SEM images showing the fracture surfaces of the weld metal region a) and the corresponding void networks b)*

3.4. *Instrumented Charpy test results*

By determining the impact energy for the base metal tested at 20 °C, a diagram was obtained, Fig.6 a), with a mixed brittle and ductile fracture surface, Fig.7 a). In order to create a crack in this zone, the measured impact energy is 28.6 J, and 5.6 J is used for propagation. The impact energy diagram for the temperature of -40 °C, Fig.6 d) shows more pronounced brittle fracture, Fig.7 d). At this temperature, the largest difference between the energy for creation in relation to the energy for crack propagation is of the highest percentage. The energy to create a crack of 27.8J slightly decreased compared to the previous temperature tests, while the crack propagation energy was significantly lower and amounted only to 1.0J. Determining the fracture energy for fusion line tested at 20°C, the diagram was obtained, Fig.6 b), with the prevailing ductile fracture surface, Fig.7 b). For creation of crack in this zone, the measured impact energy is 45.7J, and 29.6J is used for growth. Diagram of the impact energy for temperature of -40°C, Fig. 6 e) is a purely brittle fracture, Fig. 7 e). The crack creation energy of 27.7J slightly decreased compared to tests at previous temperatures, while the crack propagation energy was significantly lower and amounted to 12.3J.

By determining the impact energy for the weld metal examined at 20 °C, a diagram with a typical ductile fracture surface was obtained, Fig. 6 c) and 7 c). In order to create a crack in this zone, the measured impact energy was 29.0 J, while significantly more energy was used for crack propagation, in the amount of 55.4 J. The diagram of energy impact for the temperature of -40 °C, Fig. 6 f) and 7 f) is a ductile fracture. The energy to create a crack of 24.2 J significantly decreased compared to tests at previous temperatures, while the crack propagation energy was slightly lower and amounted to 37.3 J.

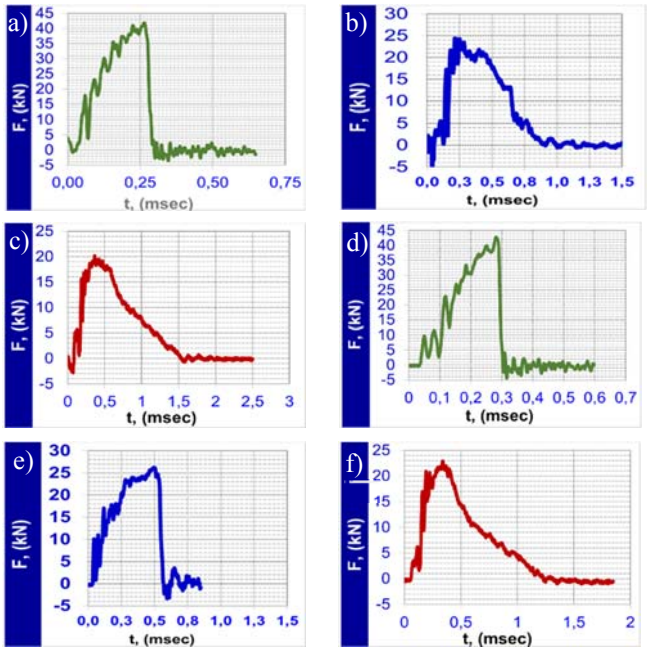

a) base metal, b) HAZ and c) weld metal. The load-time (F-t) curve recorded by oscilloscope of Charpy impact specimens fractured at -40 °C d) base metal, e) HAZ and f) weld metal.

Fig. 6. *The load-time (F-t) curve recorded by oscilloscope of Charpy impact specimens fractured at 20 °C*

4. DISCUSSION

It is known that welded joints are very heterogeneous, since they include weld metal, heat affected zone and base metal. Hardness is therefore defined by the zone of minimum hardness, which in the case of armor steel welding with austenitic filler material, is the weld metal zone. The tensile strength achieved in this research of 833 MPa is rather high for austenitic filler material and significantly higher than the tensile strength obtained by low austenite consumable, [9].

The impact energy value at all temperatures indicates that the crack propagation was very difficult. However, it can be concluded that there has been a pronounced drop in the impact energy with a drop in the test temperature. With a decrease in temperature from 20 °C to -40 °C, the energy impact drop is from 75.3 J to 40.0 J. At a temperature of 20 °C, the ratio of energy for initiation and propagation is

70:30. On the energy - time curve, after the initiation energy, a mild drop occurred, which indicates that more energy was needed for crack propagation. The impact energy data can be linked to the obtained hardness values measured around the fusion line, as the impact energy increases with the decrease in the hardness value. Fracture area fractography at -20 °C and -40 °C shows the prevailing brittle fracture.

Reducing the impact energy in the weld metal from 84.4 J to 64.4 J, obtained at temperatures of 20 °C and -40 °C, is noticeable. A large drop is characteristic of ductile materials, [10] because at lower temperatures, the energy needed to crack propagation is reduced. The SEM tests showed ductile fracture at all test temperatures. On the load - time curve, after the energy for initiation, a very slight drop, characteristic of ductile fracture, occurred. When it comes to temperatures of -40 °C, the ratio of energy for propagation and crack initiation remained the same, 34:66% in favor of propagation energy. After achieving the initiation energy of 20.8 J, there is a slight fall in the curve and the required energy for propagation is 40.7 J. The impact energies at temperatures of -40 °C and 20 °C are achieved due to an optimum hardness of 200 HV and high content of nickel and manganese. At a temperature of -40 °C, the initiation energy decreased considerably, but still remained high. SEM microscopy indicates that the fracture was ductile at all investigated temperatures. In relation to the metallography shown in the study, [9] segregated δ - ferrite is noticeable, while in the results of this work it is evenly distributed, which can be the cause of higher impact energy regarding both tests. Thicker and more uniform arrangement of δ -ferrite was obtained by the REL method compared to the MIG procedure, [[11]]. The amount of δ - ferrite measured in this test is approximately the same with REL welding in the study with the notion that the arrangement of δ - ferrite in this test is even more uniform.

The selected interpass temperature and preheating temperature yielded a lower quantity of diffused hydrogen compared to the preheating temperature of 80 °C, where the obtained value was 0.5 ml/100 g [2]. The quantity of residual hydrogen of 0.06 ml/100 g obtained with the interpass temperature and preheating temperature of 160 °C and 150 °C, respectively, was expected considering the higher quantity of diffused hydrogen. The quantity of residual hydrogen is significantly lower than the value of 8.0 ml/100 g obtained with the preheating temperature of 80°C.

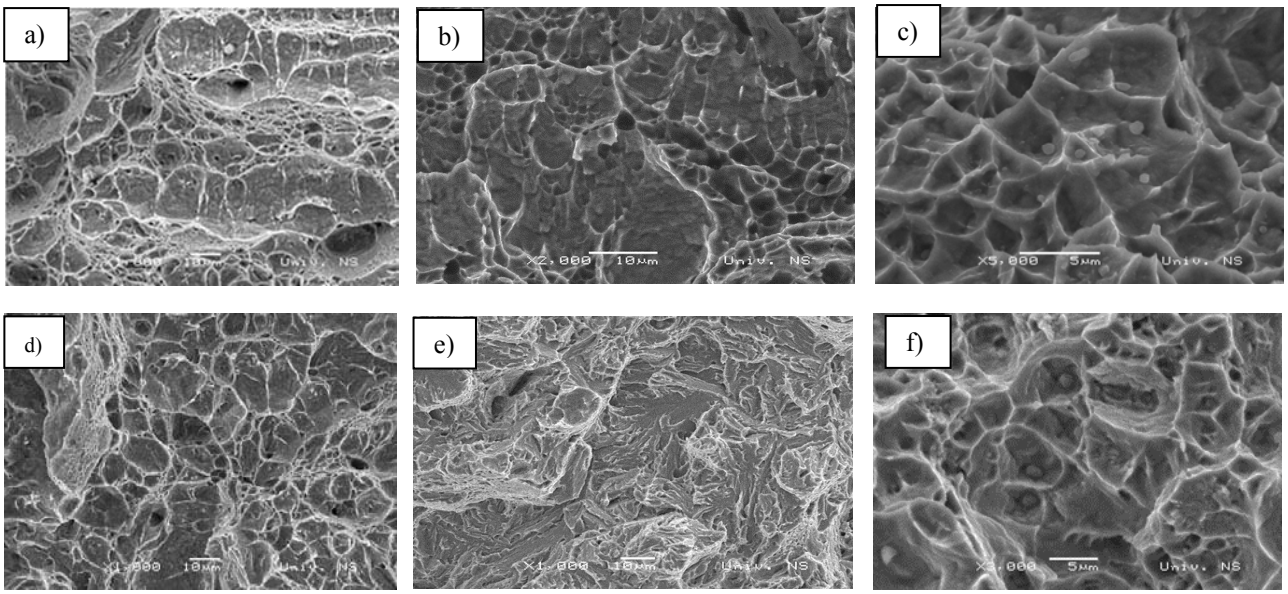

Fig 7. *SEM fractograph of Charpy impact specimens fractured at 20 °C a) base metal, b) HAZ and c) weld metal. SEM fractograph of Charpy impact specimens fractured at -40 °C d) base metal, e) HAZ and f) weld metal.*

5. CONCLUSIONS

On the basis of the results presented in this work, the following conclusions may be made:

1. A solid wire preheated at 150 °C and 160 °C provides welded joints with a low amount of diffusible and residual hydrogen. Compared to the standard preheating temperature of 80 °C, the higher interpass and preheating temperatures contribute to lower amounts of diffusible and residual hydrogen.
2. Tensile strength of weld metal in the specimen welded with austenitic filler metal reached 833 MPa, which is greater than results published for the same filler metal in researches of manual welding.
3. Austenitic filler material shows a significant decrease in impact energy, followed by reduction in testing temperature. The results at room temperature showed high energies for crack initiation 56 J and propagation 29 J. The results at -40 °C indicate that significantly less energy is required for crack initiation 41 J, while a small drop was observed for propagation 21 J. During

SEM analysis of the fracture surface, small high density dimples were clearly visible. Morphology of the fracture surface at -40 °C indicates a mixed brittle ductile fracture. The results at room temperature showed high energy absorptions for crack initiation (48 J) and propagation (27 J). The results at -40 °C indicated that significantly less energy is required for crack initiation (29 J) and propagation (11 J). The lowest energy for initiation (30 J) and crack propagation (5 J) at room temperature has a base metal. In this zone, a slight decrease in the energy of the impact between the test temperature of 20 °C and -40 °C.

ACKNOWLEDGMENTS

The authors would like to thank Dr. Zijah Burzic and the Military Technical Institute for mechanical testing.
This study was financially supported by the Ministry of Education, Science and Technological Development of the Republic of Serbia through Project No. ON 174004.

REFERENCES

[1] Mazar Atabaki, M, Ma J, Yang, G Kovacevic R. Hybrid laser/arc welding of advanced high strength steel in different butt joint configurations. *Mater Des* 2014; 64: 573–587.

[2] Kuzmikova L, Norrish J, Callaghan M. Research to establish a systematic approach to safe welding procedure development using austenitic filler material for fabrication of high strength steel. In: *16th International Conference on the Joining of Materials*. 2011, pp. 1–13.

[3] Lucon E. Estimating dynamic ultimate tensile strength from instrumented Charpy data. *Mater Des* 2016; 97: 437–443.

[4] Cabrilo A, Geric K. Weldability of High Hardness Armor Steel. *Adv Mater Res* 2016; 1138: 79–84.

[5] EN ISO 3690-2012 Weldability of High hardness armour steel, in Advance Material Research. 2012.

[6] ISO 4136:2012 - Destructive tests on welds in metallic materials - Transverse tensile test. 2012.

[7] EN ISO 5817:2014Welding - Fusion-welded joints in steel, nickel, titanium and their alloys (beam welding excluded) -- Quality levels for imperfections. 2014.

[8] Department of defense manufacturing process standard. MIL-STD-1185: Welding, high hardness armor. 2008.

[9] Magudeeswaran G, Balasubramanian V, Madhusudhan Reddy G. Effect of welding processes and consumables on fatigue crack growth behaviour of armour grade quenched and tempered steel joints. *Def Technol* 2014; 10: 47–59.

[10] Hu J, Du LX, Xu W, et al. Ensuring combination of strength, ductility and toughness in medium-manganese steel through optimization of nano-scale metastable austenite. *Mater Charact* 2018; 136: 20–28.

[11] Magudeeswaran G, Balasubramanian V, Sathyanarayanan S, et al. Dynamic Fracture Toughness of Armour Grade Quenched and Tempered Steel Joints Fabricated Using Low Hydrogen Ferritic Fillers. *J Iron Steel Res Int* 2010; 17: 51–56.